SUPPORTING INFORMATION

Glucose and maltose surface functionalized thermoresponsive poly(N-vinylcaprolactam) nanogels

Joonas Siirilä, Sami Hietala, Filip S. Ekholm, Heikki Tenhu

Department of Chemistry, University of Helsinki, FINLAND

Table of content

NMR-spectra of Glc-N_3 2
NMR-spectra of Glc-TEG-N_3 3
NMR-spectra of Mal-N_3 4
NMR-spectra of Glc-TEG-N_3 5
Kinetics of PNVCL nanogel synthesis 6
^{1}H-NMR spectrum of PA 7
^{1}H-NMR spectrum of PNVCL nanogel 8
^{1}H-NMR spectrum of PNVCL-TEG-Glc 9
^{1}H-NMR spectrum of PNVCL-Mal 10
^{1}H-NMR spectrum of PNVCL-TEG-Mal 11
Kinetics of a sugar functionalization of PNVCL-PA nanogel 12
^{1}H-NMR spectrum of PNVCL-Glc prepared via CuAAC in D_2O 13
Size distributions (CONTIN) of PNVCL-sugars at 25 ^oC 14

Hydrodynamic size of PNVCL-sugars as a function of temperature 14
Salt induced aggregation at 50 °C.....15

NMR-spectra of Glc-N_3

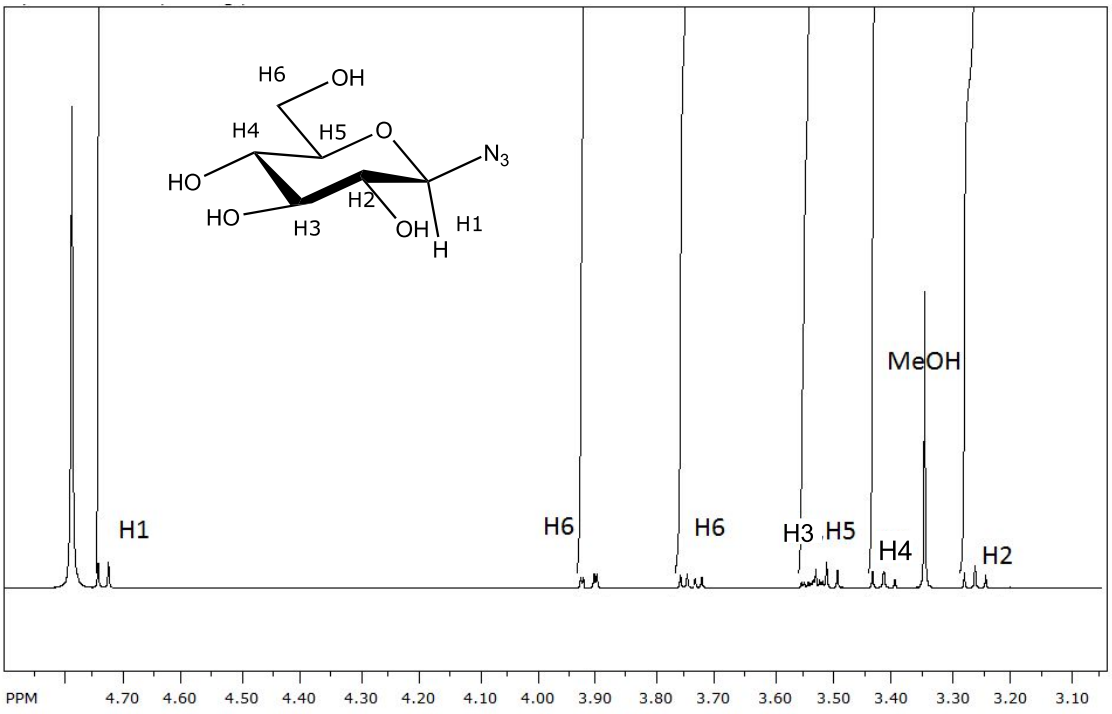

Figure S1. ^{1}H-NMR spectrum of Glc-N_3

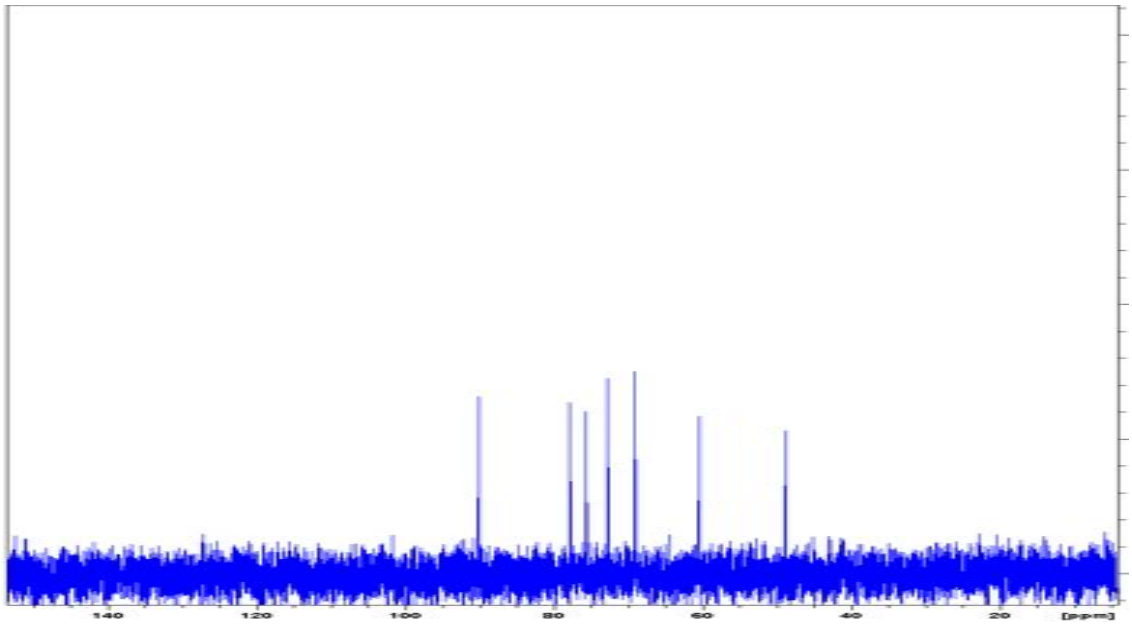

Figure S2. ^{13}C-NMR spectrum of Glc-N_3

NMR-spectra of Glc-TEG-N_3

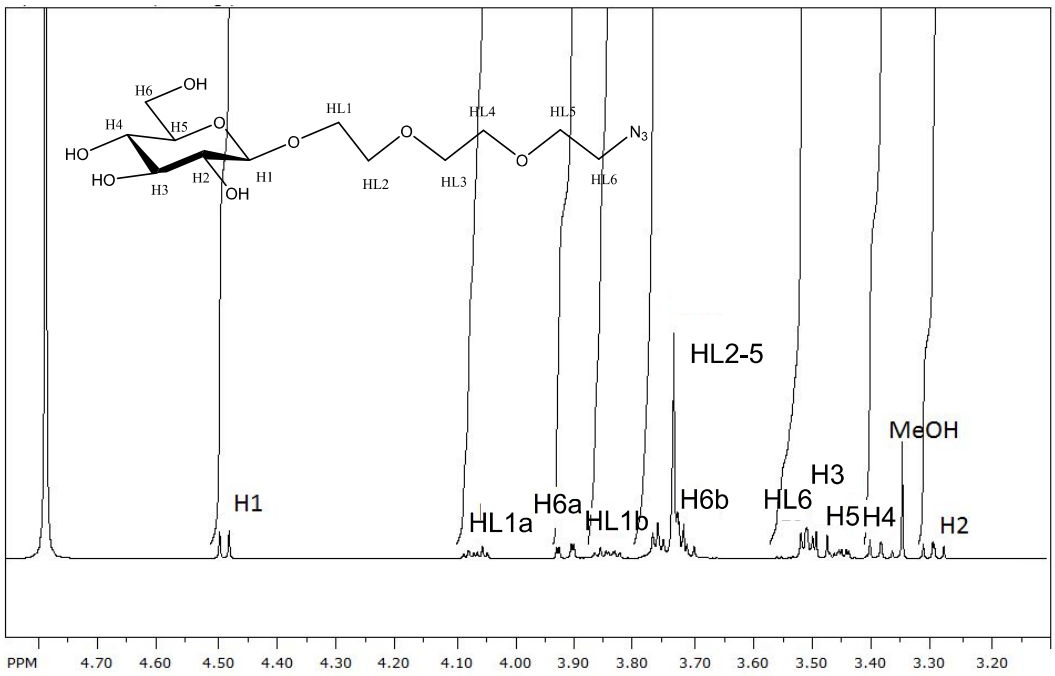

Figure S3. ^{1}H-NMR spectrum of Glc-TEG-N_3.

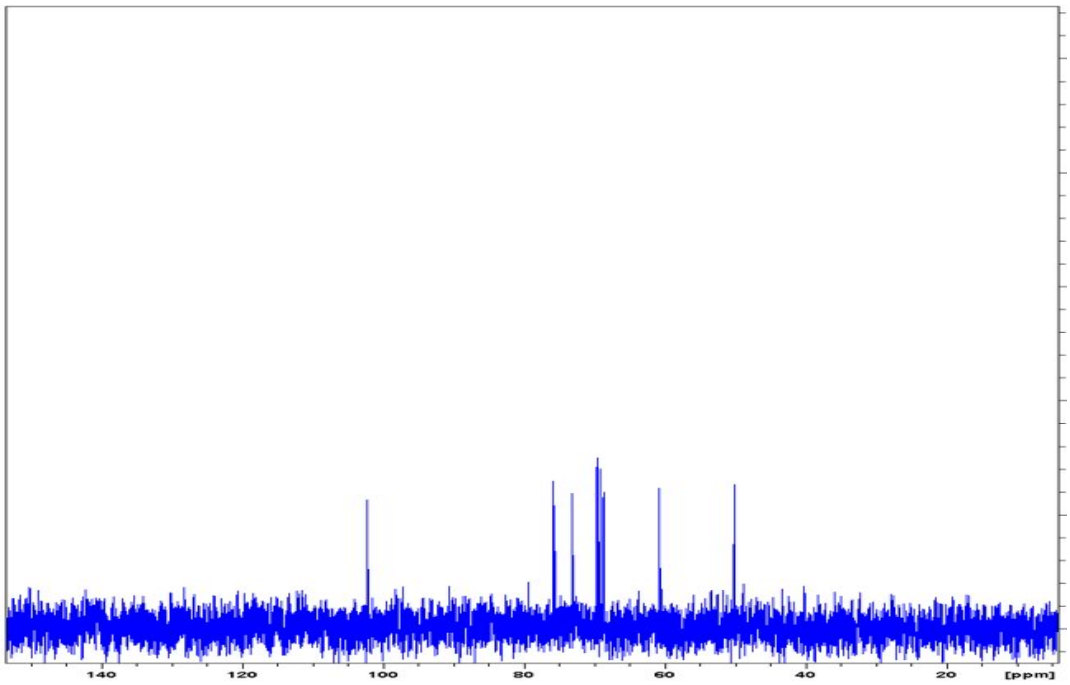

Figure S4.[13]C-NMR spectrum of Glc-TEG-N_3.

NMR-spectra of Mal-N_3

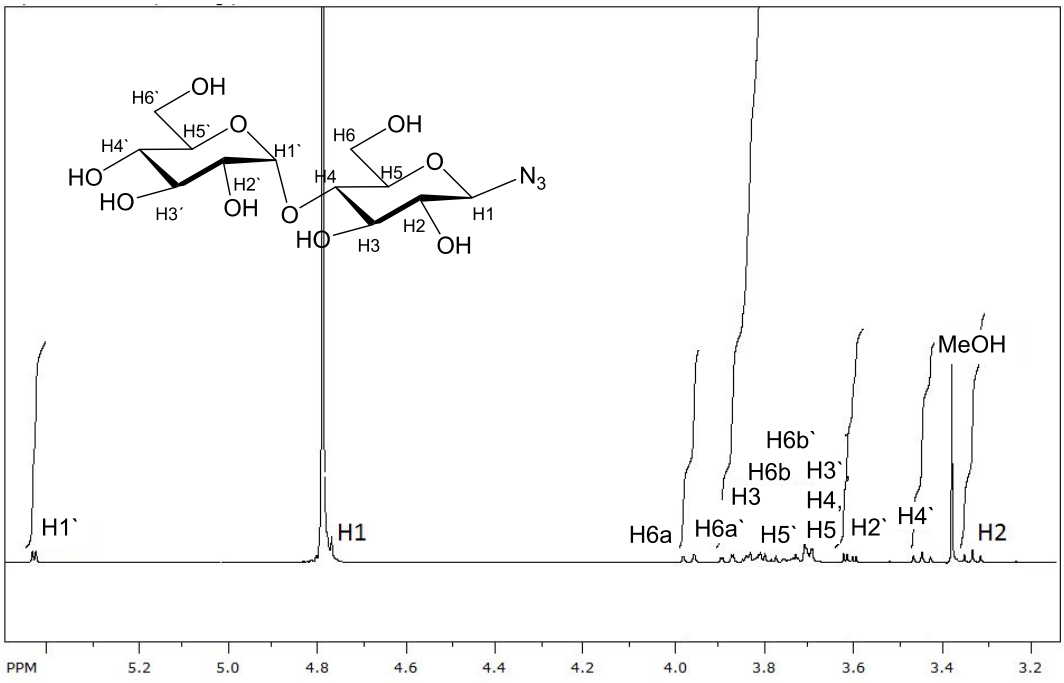

Figure S5. [1]H-NMR spectrum of Glc-TEG-N_3.

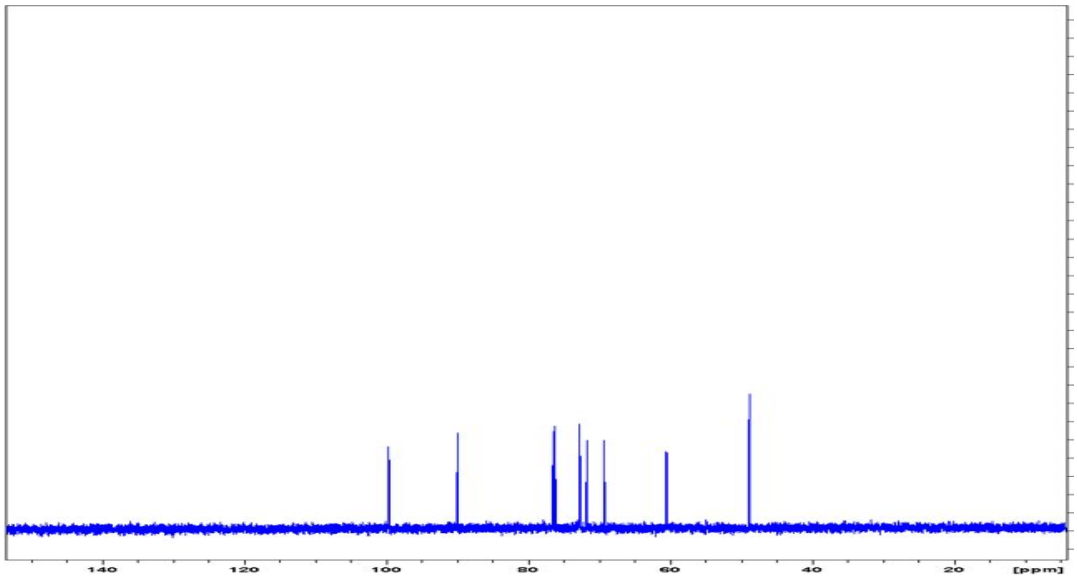

Figure S6.[13]C-NMR spectrum of Glc-TEG-N_3.

NMR-spectra of Glc-TEG-N_3

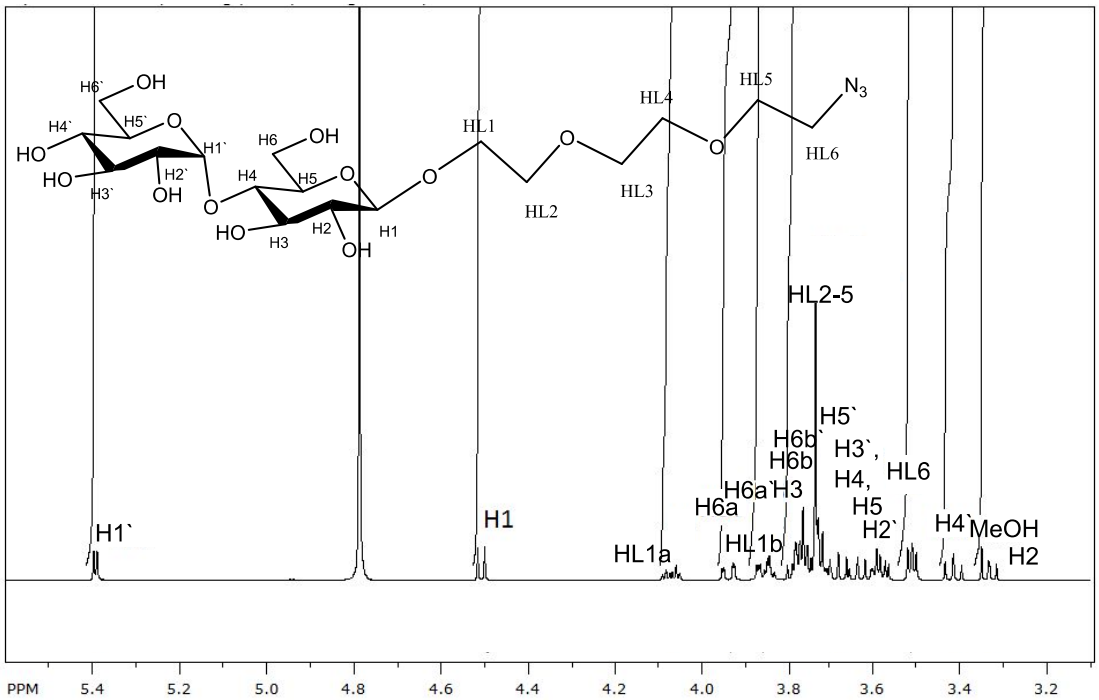

Figure S7. [1]H-NMR spectrum of Glc-TEG-N_3**.**

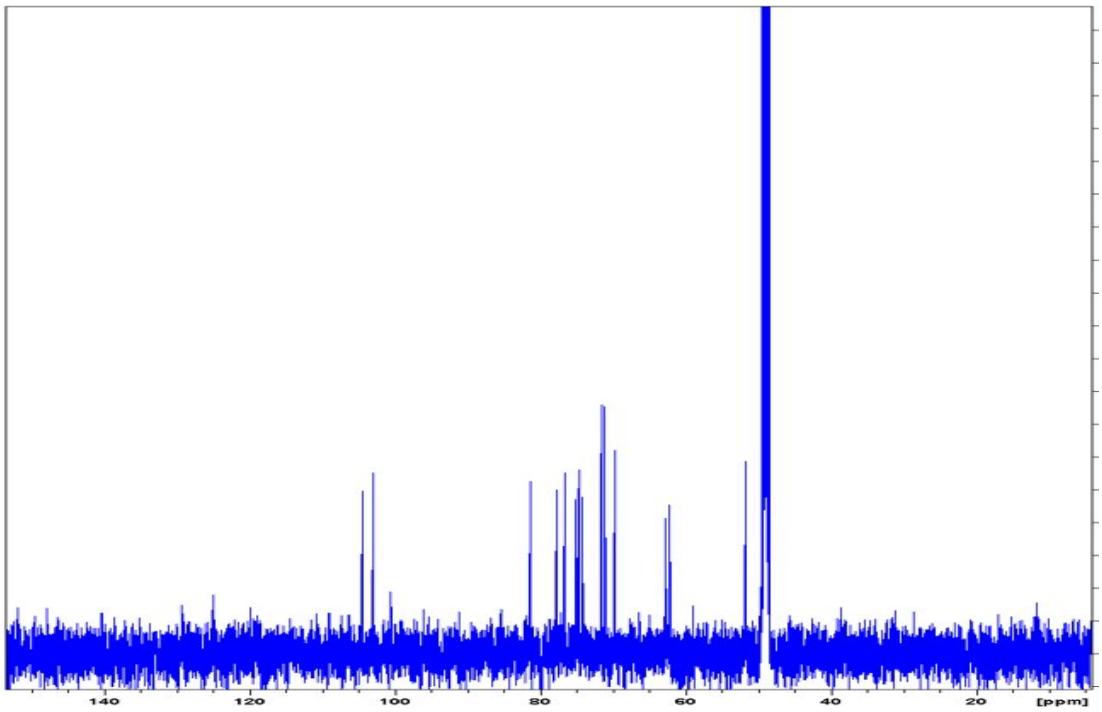

Figure S8.[13]C-NMR spectrum of Glc-TEG-N_3.

Kinetics of PNVCL nanogel synthesis

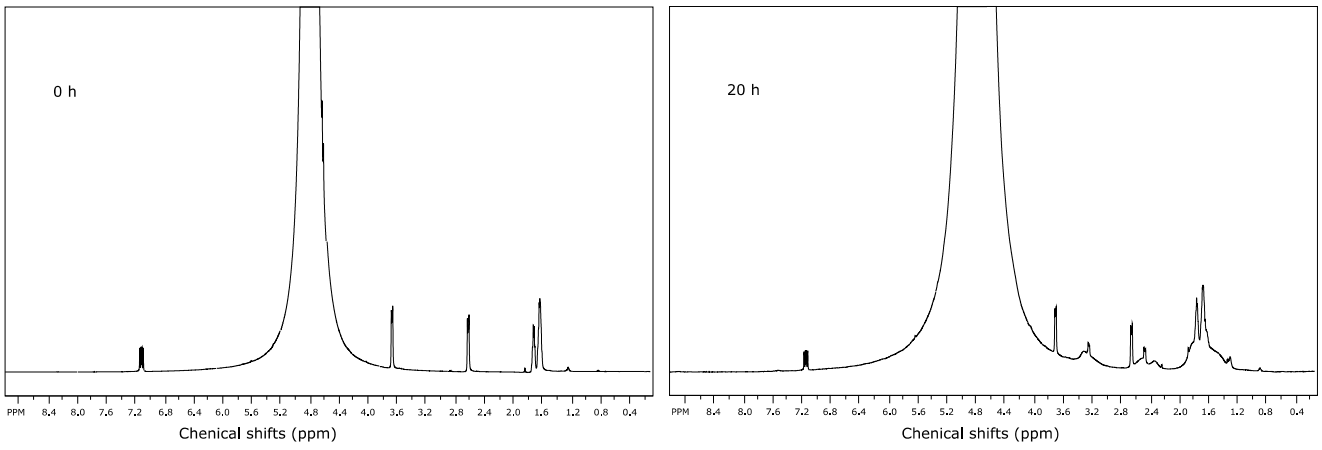

Figure S9. [1]H-NMR spectrum of conversion sample taken after 0h (left) and after 20h (right)

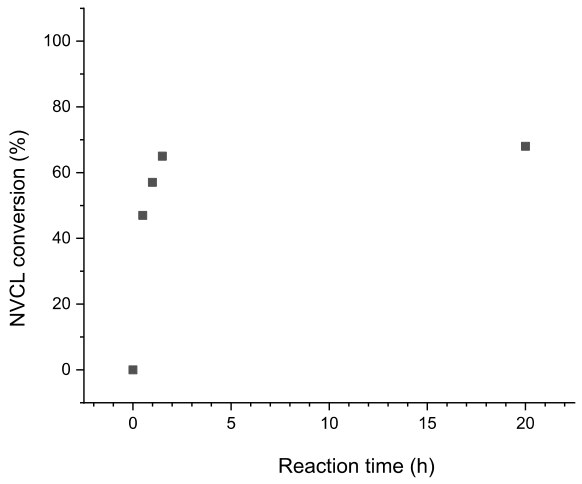

Figure S10. Kinetics of the polymerization according to ^{1}H-NMR

^{1}H-NMR spectrum of PA

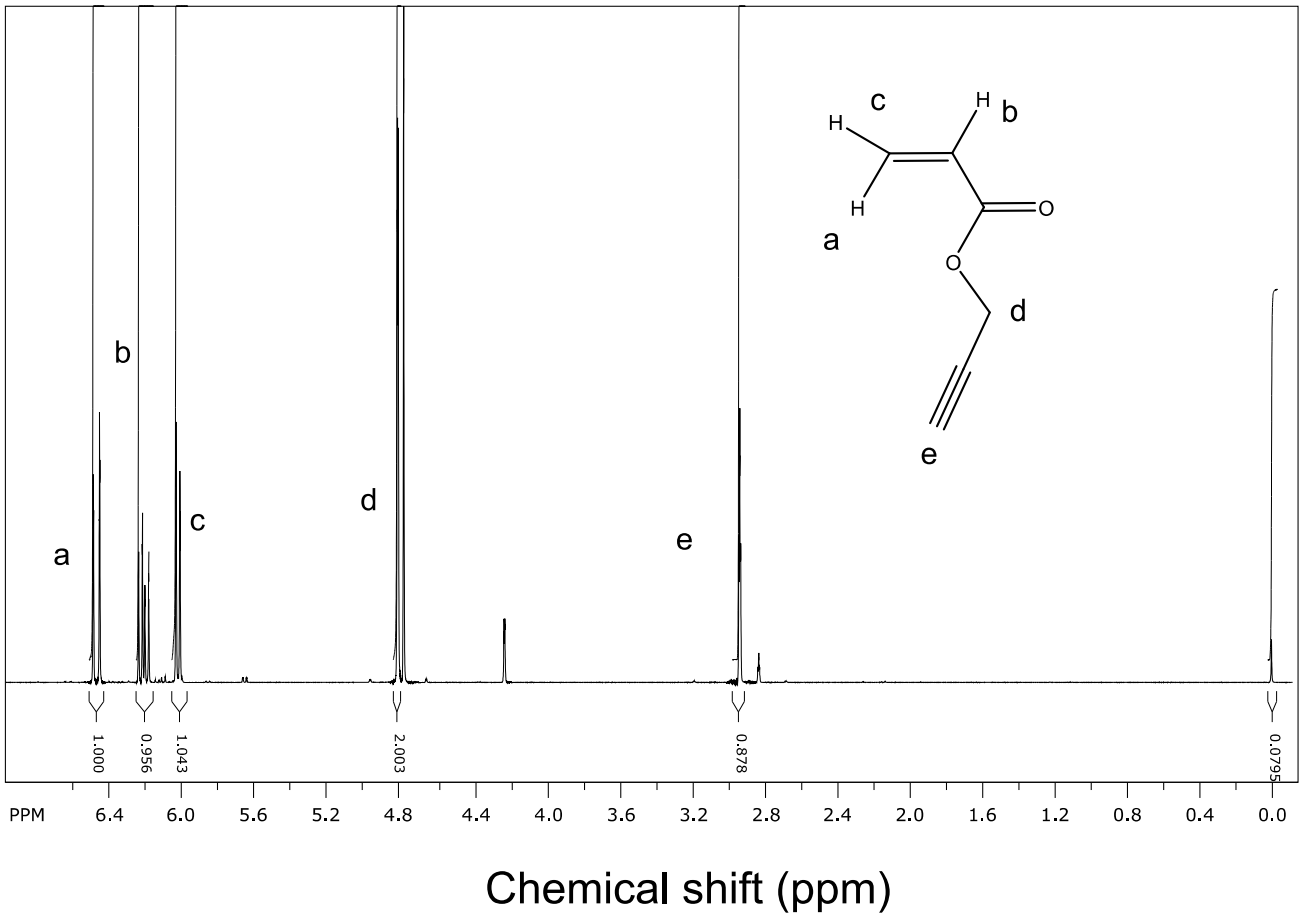

Figure S11. ^{1}H-NMR spectrum of PA in D_2O

^{1}H-NMR spectrum of PNVCL nanogel

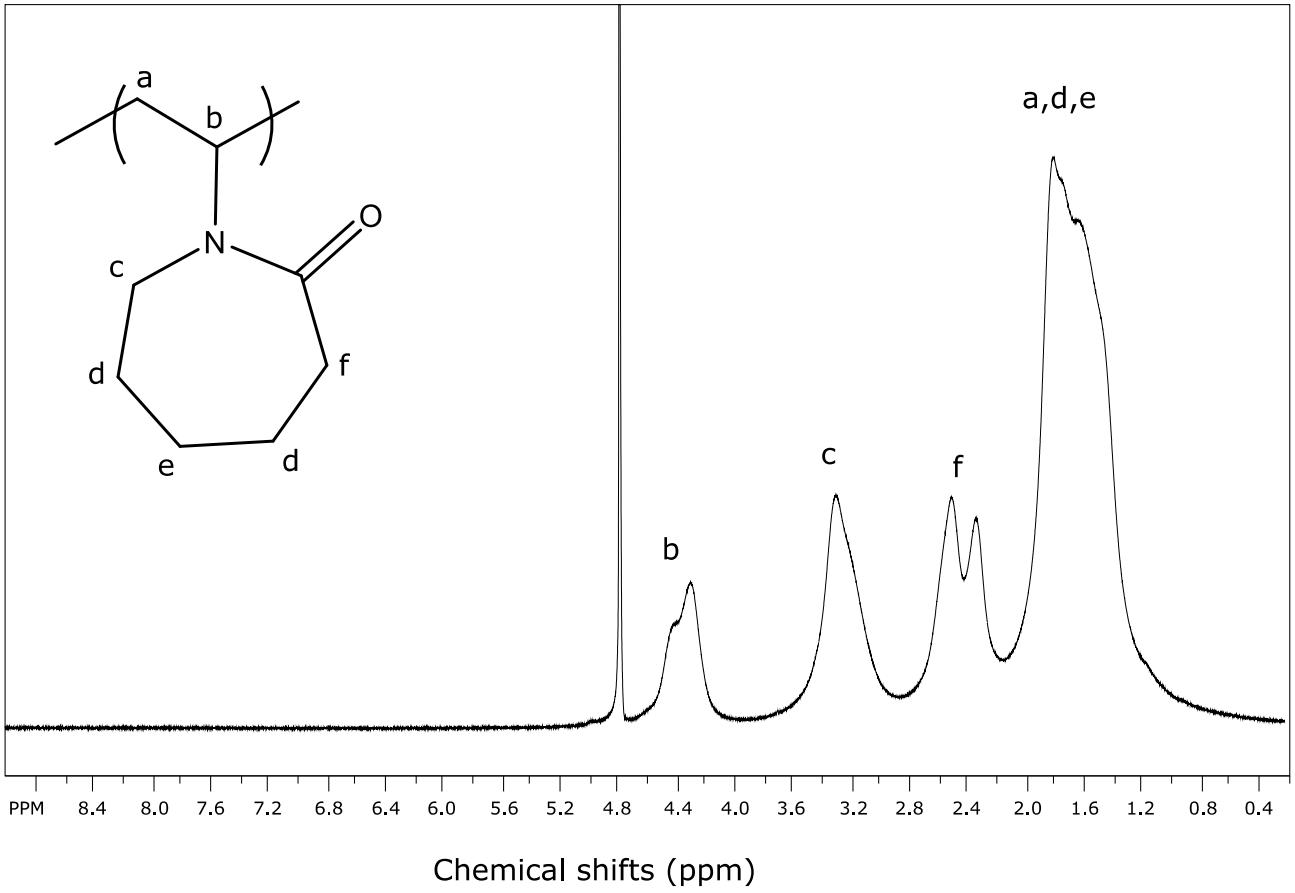

Figure S12. ^{1}H-NMR spectrum of PNVCL nanogel

^{1}H-NMR spectrum of PNVCL-TEG-Glc

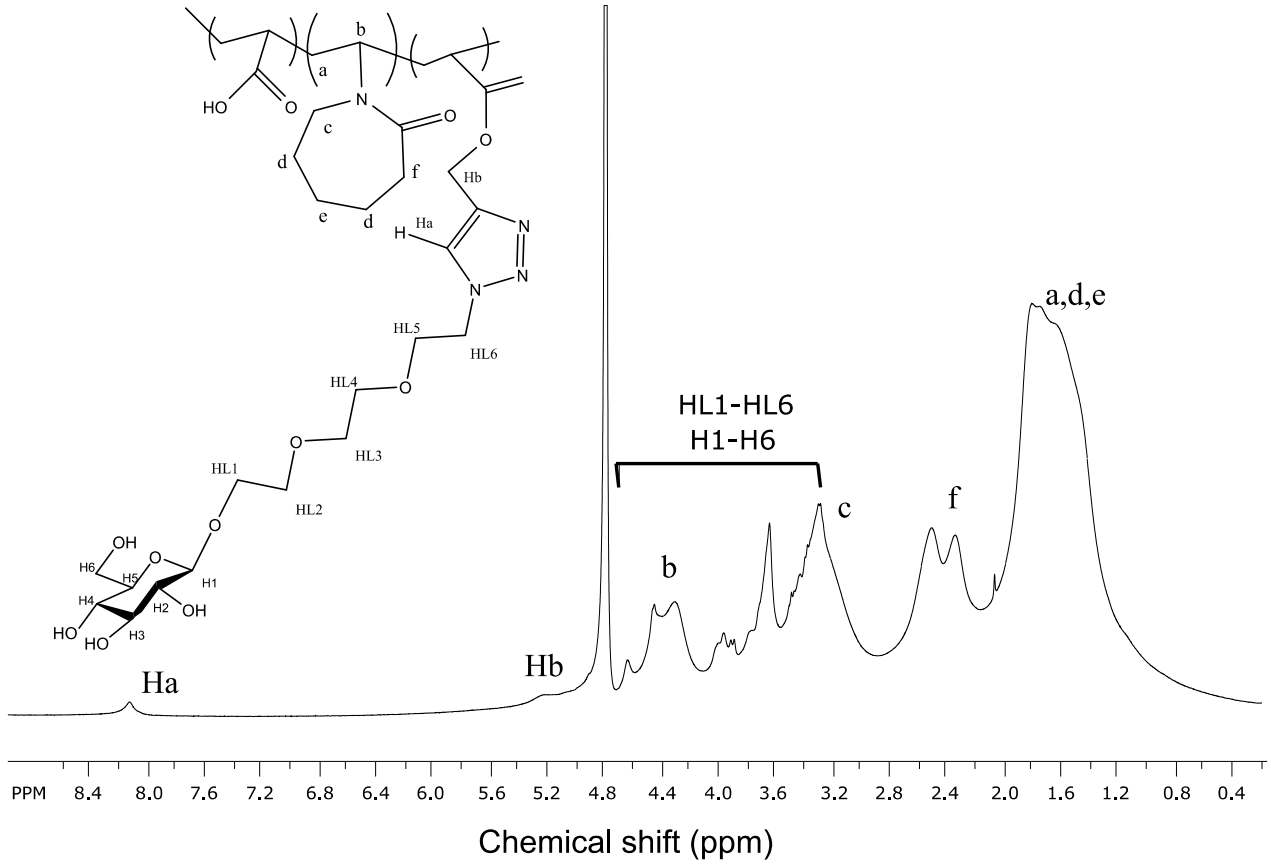

Figure S13. ^{1}H-NMR spectrum of PNVCL-TEG-Glc

^{1}H-NMR spectrum of PNVCL-Mal

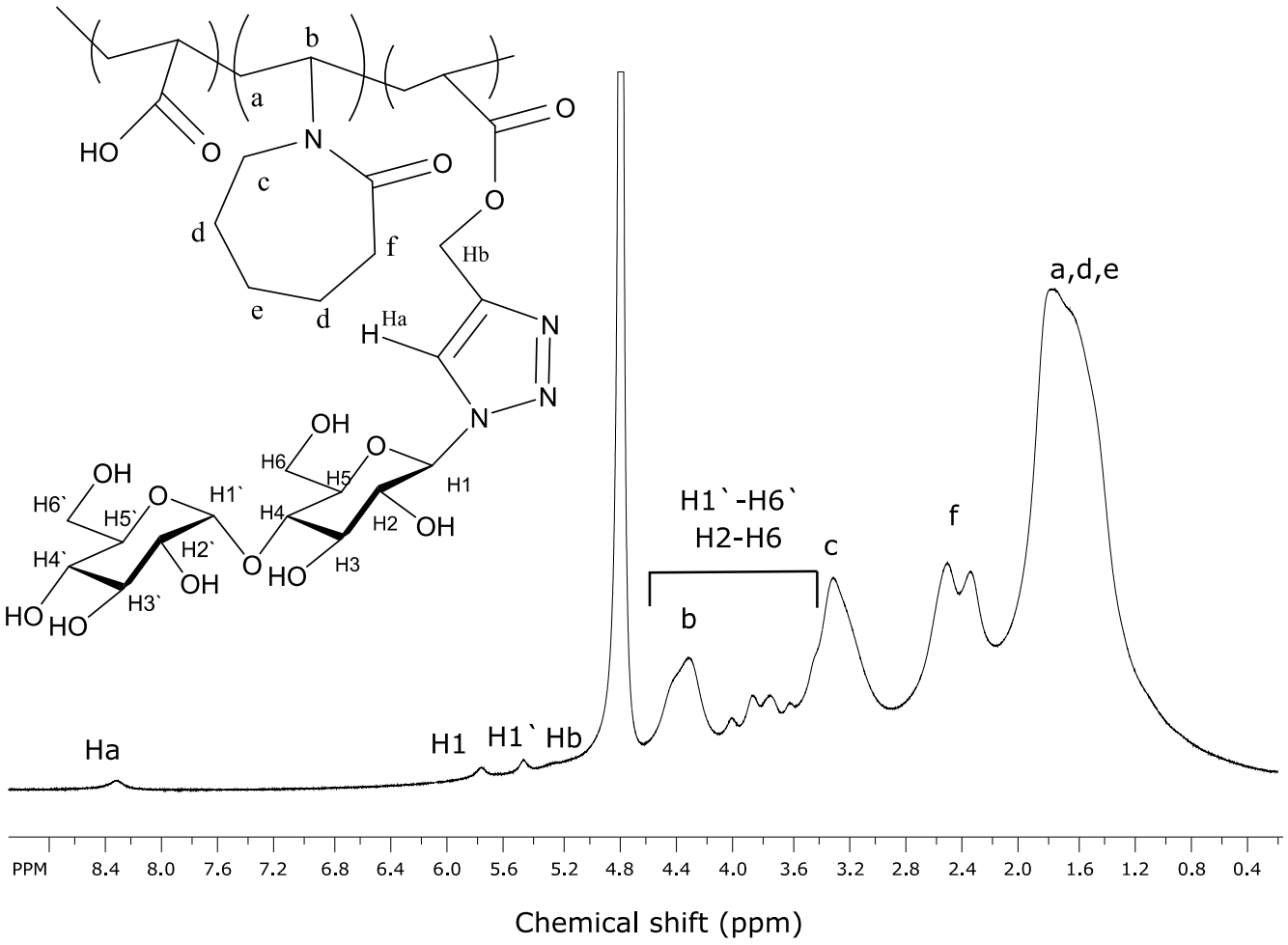

Figure S14. ^{1}H-NMR spectrum of PNVCL-Mal

^{1}H-NMR spectrum of PNVCL-TEG-Mal

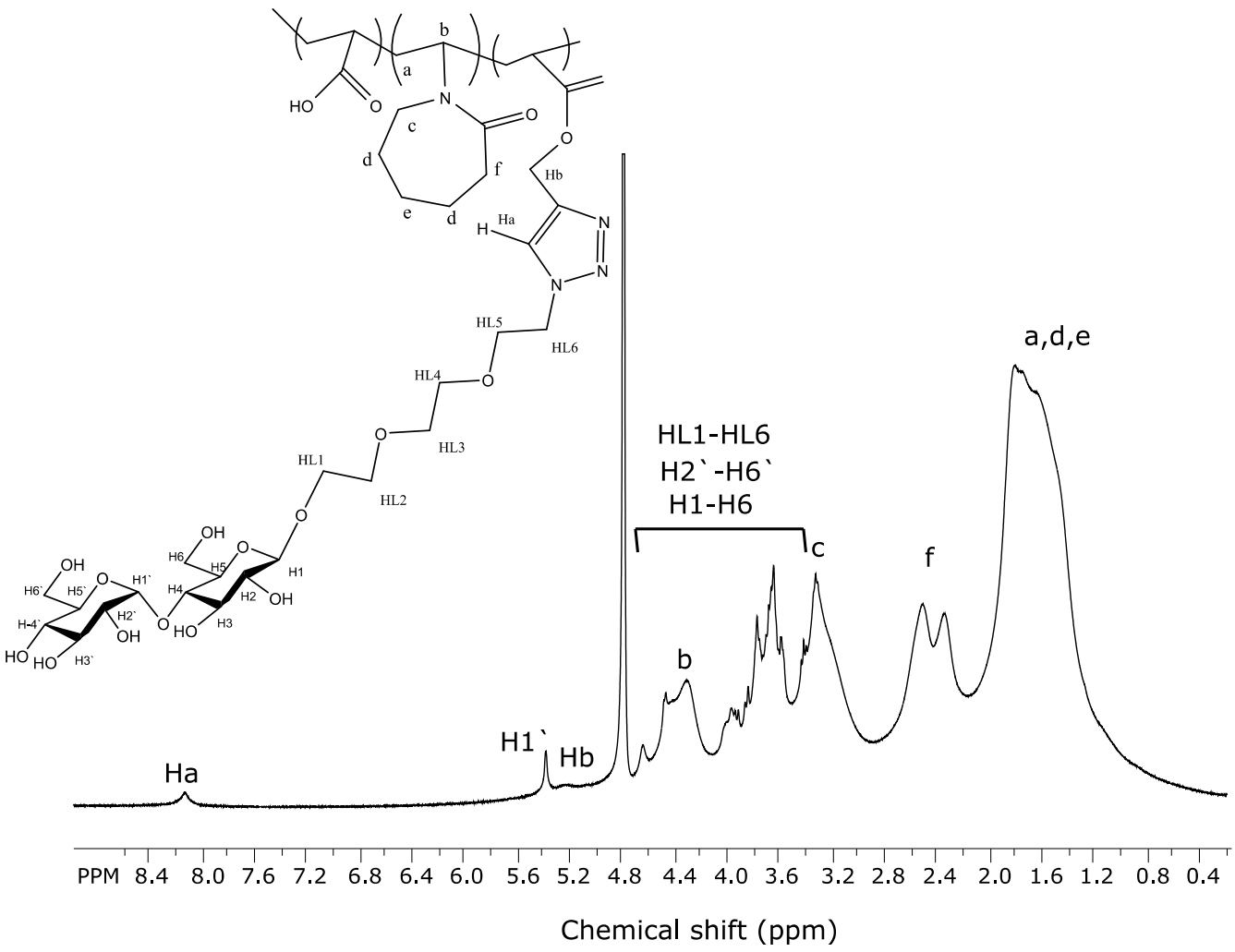

Figure S15. ^{1}H-NMR spectrum of PNVCL-TEG-Mal

Kinetics of a sugar functionalization of PNVCL-PA nanogel

To make sure that the reaction time was long enough, a replica of the conjugation reaction to obtain PNVLC-Glc was performed in D_2O and followed with ^{1}H-NMR. The intensity of a peak at 5.8 ppm, was used to follow the reaction (^{1}H-spectrum of PNVCL-Glc with peak assignations is presented in main article Figure 6) and results are presented in Figure S12. It is seen that the reaction has happened during 8 h. ^{1}H-NR of the purified product is presented in Figure S13. The nanogel synthesized in D_2O differs from the PNVCL-Glc nanogel, as there is a deuterium ion instead of a proton attached to the triazole ring. Akula et al. have studied this phenomenon of CuAAc reactions in D_2O as “a efficient route for the synthesis of deuterated 1,2,3-triazoles”.[S1]

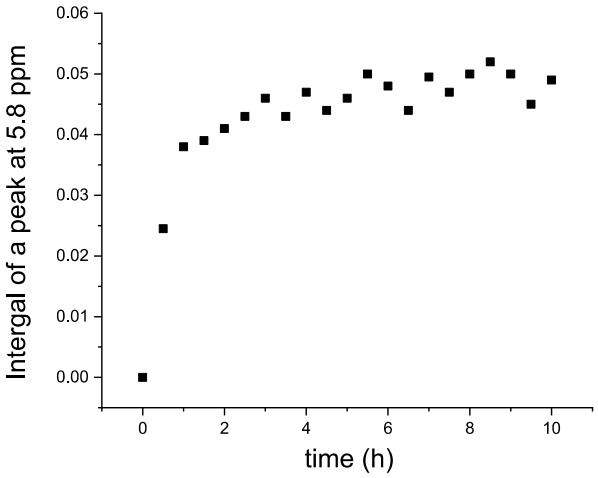

Figure S16. Kinetic of reaction between Glc-N_3 and PNVL-PA nanogel based on a ^{1}H-NMR-experiment

S1. Akula HK, Lakshman MK. Synthesis of deuterated 1,2,3-triazoles. *The Journal of organic chemistry*. 2012;77(20):8896

^{1}H-NMR spectrum of PNVCL-Glc prepared via CuAAC in D_2O

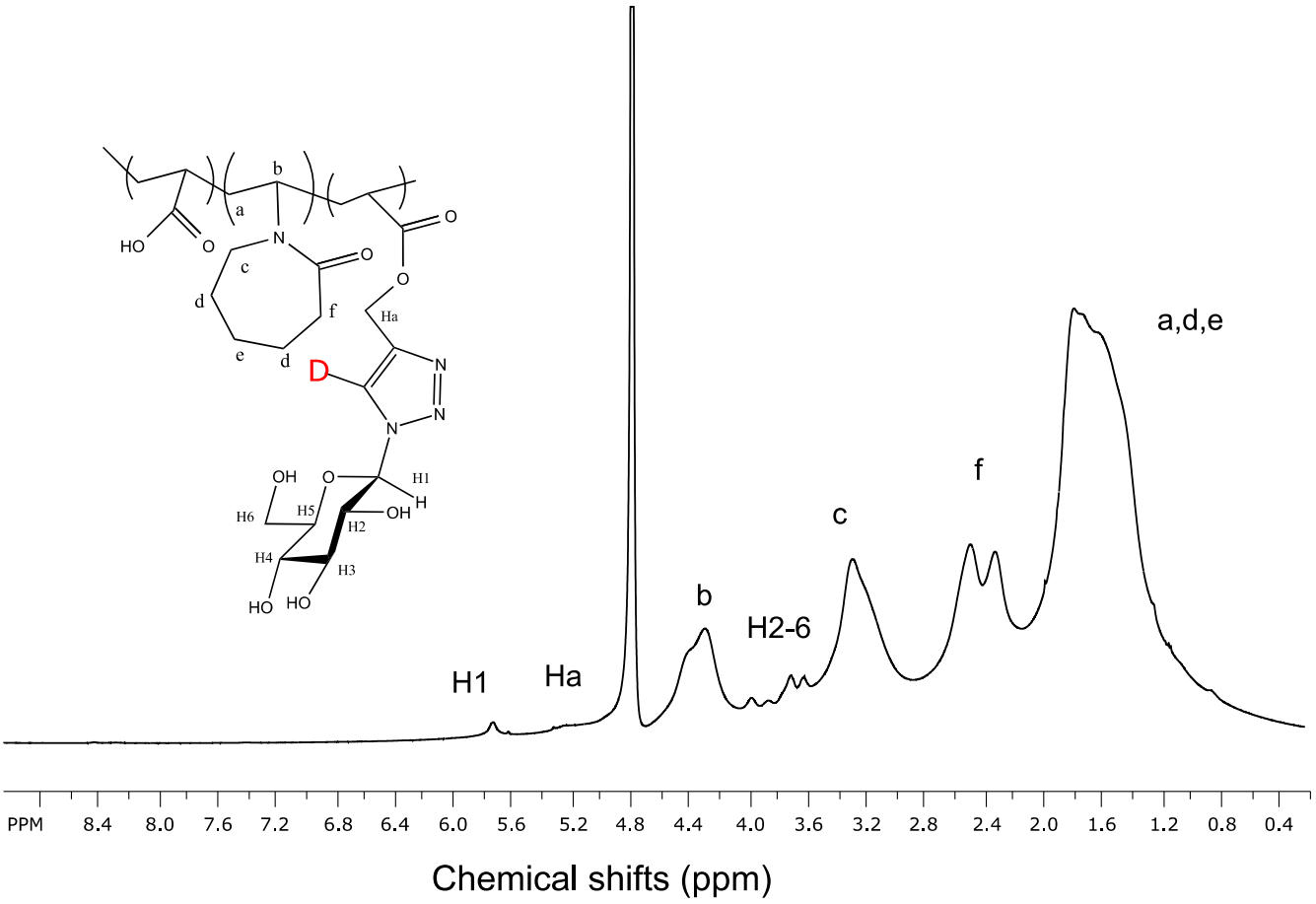

Figure S17. 1H-NMR spectrum of PNVCL-Glc prepare via CuAAC in D2O

Size distributions (CONTIN) of PNVCL-sugars at 25 ºC

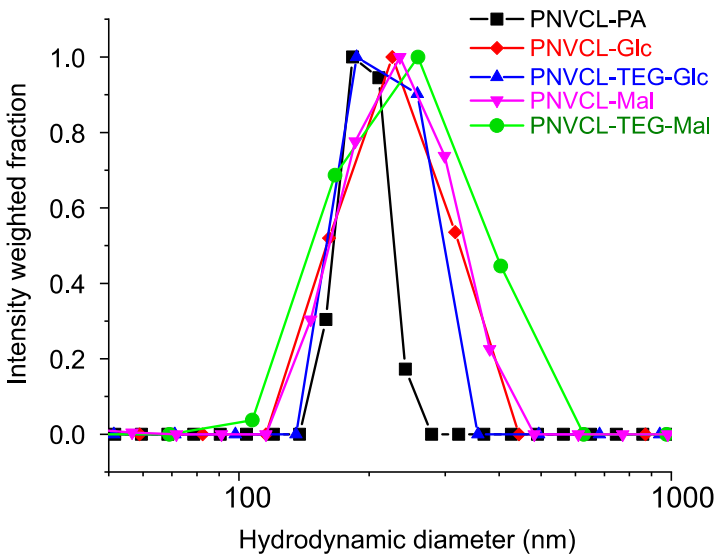

Figure S18. Hydrodynamic size distributions (CONTIN) of selected nanogels; 0.25 mg/ml in 10 mM HEPES (pH=7.4) at 25 °C

Hydrodynamic size of PNVCL-sugars as a function of temperature

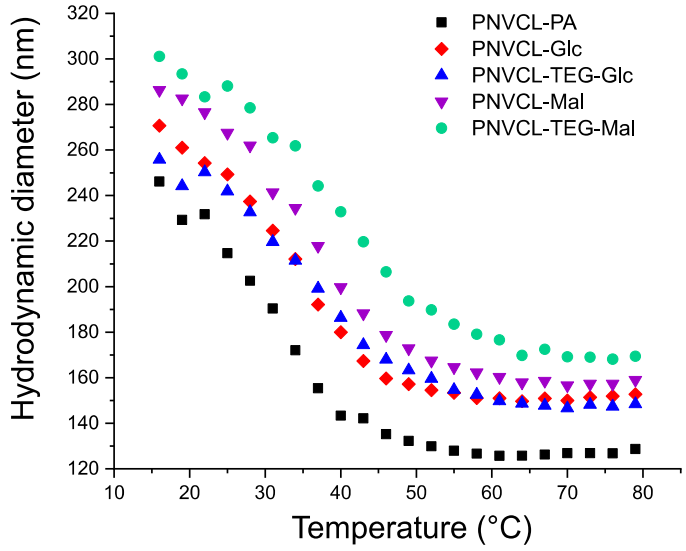

Figure S19. Hydrodynamic mean size of selected nanogels as functions of temperature; 0.25 mg/ml in 10 mM HEPES (pH=7.4) at 25 °C

Salt induced aggregation at 50 °C

Selected salt induced aggregation tests are shown Figure S16. Two points were obtained from each curve C_1 and C_2. Aggregation concentration, C_1, was taken from the point where transmittance as a function of NaCl concentration broke the linear trend. Precipitation concentration (C_2) was determined a point, where the transmittance had increased compared to previous concentration. The increase of transmittance was due to visible aggregates sedimenting out of the solution in the given 15 min stabilization time. Both aggregation (C_1) and precipitation (C_2) concentrations are listed in table S1. In addition, size distribution of PNVCL-PA in selected NaCl concentrations was measured with light scattering, see Figure S17. There was no change in particle size before and only a moderate change above the C_1 concentration. This evidenced the gradual process of particle aggregation. First nanogels start to associate moderately at C1 and then upon further increasing the NaCl the aggregates become larger and finally the aggregates become too large to stay in solution and precipitate out of solution.

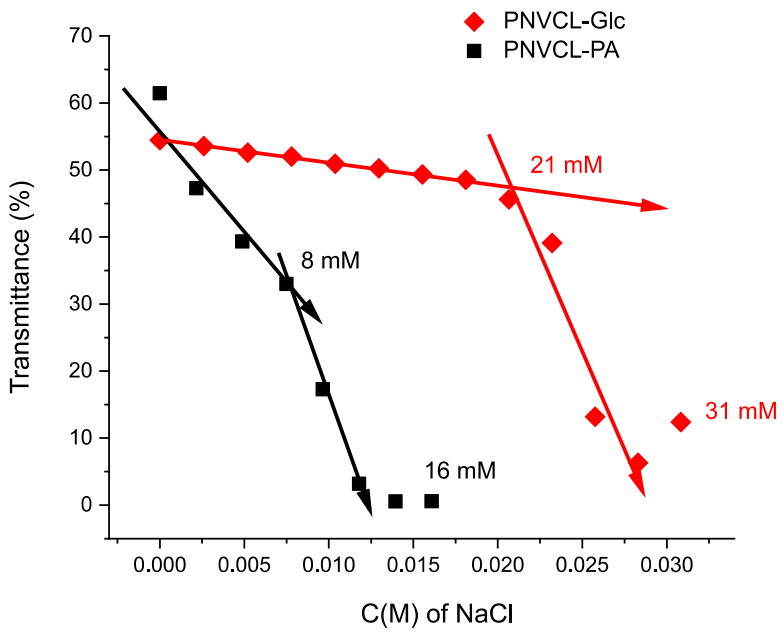

Figure S20. Salt induced aggregation of PNVCL-Glc and PNVCL-PA at 50 °C

Table. S1 Aggregation and precipitation concentrations of NaCl, see Figure S16

Product	C_1(mM) of NaCl	C_2(mM) of NaCl
PNVCL-PA nanogel	8	16
PNVCL-Glc	21	31
PNVCL-TEG-Glc	21	34
PNVCL-Mal	20	29
PNVCL-TEG-Mal	21	31

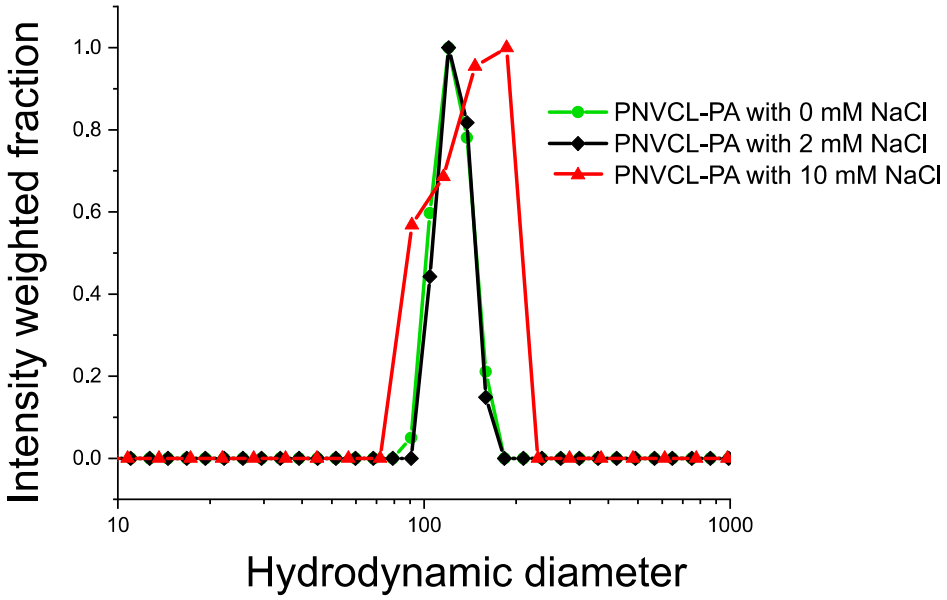

Figure S21. Size distribution of PNVLC-PA at various NaCl concetrations at 50 °C